

Qualitative aspects of the degradation of mitomycins in alkaline solution

J. H. BEIJNEN, J. DEN HARTIGH and W. J. M. UNDERBERG*

Department of Analytical Pharmacy, Subfaculty of Pharmacy, State University of Utrecht,
 Catharijnesingel 60, 3511 GH Utrecht, The Netherlands

Abstract: The major degradation product in alkaline solution of mitomycin A, mitomycin C and porfiromycin is the corresponding 7-hydroxymitosane. The isolation and the physico-chemical and analytical properties of these compounds and their derivatized analogues are discussed. Data are presented on the degradation of mitomycin C at extremely high pH values.

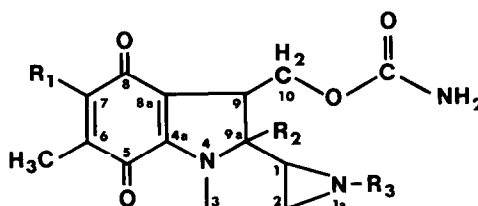
Keywords: *Mitomycin A, B and C; mitomycin degradation products in alkaline solution; 7-hydroxymitosanes; porfiromycin.*

Introduction

The unstable part of the mitomycin molecule (Fig. 1) in alkaline solution is the 7-substituent. Degradation at pH values greater than 8 leads to replacement of this function by a hydroxyl group. Although 7-hydroxymitosanes have been known for several years, only a few analytical properties of these compounds have been described [1-3].

Figure 1
 Structural formulae of several mitomycins and derivatives

	R ₁	R ₂	R ₃
Mitomycin A (MMA)	H ₃ CO	OCH ₃	H
Mitomycin B (MMB)	H ₃ CO	OH	CH ₃
Mitomycin C (MMC)	H ₂ N	OCH ₃	H
Porfiromycin (PM)	H ₂ N	OCH ₃	CH ₃
7-Hydroxy MMC (X)	HO	OCH ₃	H
7-Hydroxy PM (Y)	HO	OCH ₃	CH ₃
Acetylated MMC	H ₂ N	OCH ₃	COCH ₃
Propionated MMC	H ₂ N	OCH ₃	COC ₂ H ₅
Acetylated X	H ₃ COCO	OCH ₃	COCH ₃
Propionated X	H ₃ C ₂ OCO	OCH ₃	COC ₂ H ₅
Acetylated Y	H ₃ COCO	OCH ₃	CH ₃
Propionated Y	H ₃ C ₂ OCO	OCH ₃	CH ₃



* To whom correspondence should be addressed.

The present work describes the isolation and the physico-chemical and analytical properties of the degradation products of mitomycin C (MMC) and of porfiromycin (PM) in alkaline solution. Figure 1 represents the structural formulae of several naturally occurring mitomycins and the corresponding structures of X (the 7-hydroxy analogue of MMC), Y (7-hydroxy PM) and of their propionyl and acetyl derivatives.

Experimental

Materials

MMC was kindly provided by Prof. Dr Masaki Otagiri, Kumamoto University, Kumamoto, Japan. Mitomycin A (MMA) and mitomycin B (MMB) were supplied by Kyowa Hakko Kogyo Chemical Co., Japan and PM was supplied by Cyanamid (Pearl River, N.Y., USA). All other reagents and solvents were of analytical grade and were used as received.

Apparatus and experimental conditions

High-performance liquid chromatography. A liquid chromatograph (model M-45 solvent delivery system, Waters Associates, Milford, MA, USA) equipped with a UV 440 dual wavelength detector, operating at 313 and 365 nm, was used. A 300 × 3.9 mm i.d. stainless steel column was slurry-packed in the laboratory with 10- μ m Lichrosorb Rp-18 (Merck, Darmstadt, FRG). The following mobile phases were used: mobile phase I, methanol–water (5:95, m/m); mobile phase II, methanol–water (30:70, m/m) to which 0.5% (v/m) of a 0.5 M sodium phosphate buffer (pH 7.0) was added; mobile phase III, 1.0% (v/m) tetrabutylammonium bromide solution (20%, m/v) added to II; mobile phase IV, methanol–water (40:60, m/m) to which 1.0% (v/m) of a 0.5 M sodium phosphate buffer (pH 7.0) was added. The mobile phases were used isocratically at a flow rate of 1.0 ml/min⁻¹ with the column at ambient temperature. Samples of 10 μ l were injected.

Thin-layer chromatography (TLC). Precoated 0.25-mm silica gel plates (60 F 254 Merck) were used. About 1 μ g of an isolated decomposition product was applied on a thin-layer plate and the chromatogram was developed in a saturated chamber with chloroform–methanol (90:10, v/v). The strongly coloured compounds were detected in daylight or under UV light at 365 or 254 nm. The coloured areas were scraped off and eluted with methanol. After evaporation of the solvent, the residue was analysed by mass spectrometry (MS) or infrared (IR) spectroscopy.

Ultraviolet-visible spectrophotometry. Ultraviolet and visible spectra were recorded with a Shimadzu UV-200 double beam spectrophotometer. The pK_a was determined by absorbance measurements with a Shimadzu UV-140 double beam spectrophotometer. The 1-cm quartz cells were kept at 25°C.

Infrared spectroscopy. Infrared spectra were obtained with a Perkin–Elmer 580 B double beam ratio recording infrared spectrophotometer. A micro die KBr pellet technique was used.

Mass spectrometry. The Field Desorption (FD) mass spectra were obtained with a Varian MAT 711 double-focussing mass spectrometer, equipped with a combined

electron impact/field ionization/FD ion source and coupled to a MAT 100 data acquisition unit. 10- μm tungsten wire FD emitters containing carbon microneedles with an average length of 30 μm were used. The samples were dissolved in methanol and then loaded on the emitters by the dipping technique. An emission current of 12–20 mA was used to desorb the samples. The ion source temperature was 70°C.

Chemical ionization (CI) mass spectra were obtained using a Finnigan 3200 quadrupole mass spectrometer combined with a Finnigan 6000 data system. Methane was used as the ionizing gas. The emission current was 0.20 mA, the multiplier voltage 1800 V and the electron energy 70 eV.

Electron impact (EI) mass spectrometry was performed with a Kratos MS 80 mass spectrometer. The electron energy was 70 eV and the source temperature 200°C.

Direct current polarography. The polarographic curves were recorded on a Bruker E310 modular electrochemical system, equipped with a drop-timer and a Houston 2000 X–Y recorder. A water-jacketted 10-ml polarographic cell (Metrohm EA 880T-5) with a dropping mercury electrode, a Metrohm EA 436 Ag/AgCl/3 M KCl reference electrode and a platinum wire auxiliary electrode were employed. The cell was kept at $20 \pm 1^\circ\text{C}$. The buffer pH was measured with a Radiometer PHM-64 research pH meter, equipped with an Ingold LOT-401 combined glass reference electrode.

Isolation of X and Y components

For the isolation of microgram quantities of compounds X or Y about 1 mg of MMC or of PM respectively was dissolved in 1.0 ml of 0.1 M sodium phosphate buffer pH 11.4. These solutions were heated for 90 min at 60°C to ensure almost complete decomposition of the mitomycin to form the 7-hydroxy analogue. For MMA 20 min at 40°C was found to be sufficient for complete degradation to X.

Purification of the resulting solution was achieved by high-performance liquid chromatography using mobile phase I. The eluate containing X or Y was evaporated under nitrogen. The blue-violet residue was analysed by UV-visible spectrophotometry, HPLC, polarography and, after derivatization, by mass spectrometry, chromatography and infrared spectroscopy.

Derivatization

Derivatization of the parent mitomycin and the degradation products was performed at ambient temperature for 1 h with acetic anhydride — or propionic anhydride—pyridine mixtures (5:1, v/v).

After evaporation of the solvents under nitrogen the coloured residue was dissolved in methanol and purified on thin-layer plates of silica gel.

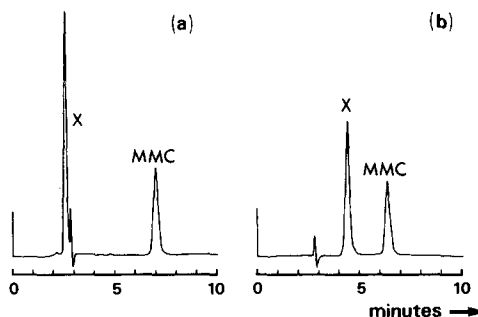
Results and Discussion

Chromatography

Figures 2a and 2b show typical chromatograms of a decomposition mixture of MMC at about one half-life. With mobile phase II (Fig. 2a), X is eluted before the solvent front. The anionic character of X at pH 7 is demonstrated by the retention achieved by adding a quaternary ammonium pairing ion to the mobile phase (Fig. 2b).

When an eluent with a very high water concentration (mobile phase I) is used, X shows some retention (capacity ratio, $k' = 0.3$); this appears to be sufficient for isolation

Figure 2
HPLC chromatograms of a decomposition mixture (3×10^{-5} M MMC) at about the half-life: (a) mobile phase II; (b) mobile phase III; detection at 365 nm. For chromatographic conditions; see text.



purposes. With a sufficiently acidic mobile phase, X is quantitatively protonated; both this compound and MMC are eluted as tailing peaks owing to on-column degradation.

Acetylation or propionation of X or Y results in the formation of strongly lipophilic compounds. The chromatographic behaviour of these derivatives and the naturally occurring mitomycins in terms of k' (mobile phase IV) and R_f values (mobile phase: chloroform–methanol, 90:10 v/v) are listed in Table 1. Comparison of the data obtained from reversed phase liquid chromatography and normal phase TLC shows that introduction of a methyl, acetyl or propionyl group on the aziridine nitrogen mainly influences the hydrophilicity. In contrast, the substituent at the 7-position mainly influences the hydrophobicity of the molecule.

Table 1
Column capacity ratios (k') and R_f values of several mitomycins and derivatized degradation products

Solute	k'^*	R_f^\dagger
MMA	3.4	0.31
MMB	1.43	0.28
MMC	0.73	0.12
PM	1.06	0.28
Acetylated MMC	1.12	0.29
Propionated MMC	1.73	0.38
Acetylated X	3.7	0.47
Propionated X	13.2	0.51
Acetylated Y	3.7	0.54
Propionated Y	7.6	0.57

* Mobile phase IV.

† Solvent system: chloroform–methanol (90:10, v/v).

Absorption spectrophotometry

MMC and deprotonated X in methanol and water show related ultraviolet absorption spectra with maxima near 360 nm. Protonation of the 7-enolate group is coupled with a hypsochromic shift in the UV spectrum. Fast degradation of X in an acidic medium allows only estimates to be made of $A_{1\text{ cm}}^{1\%}$ and of the wavelengths of maximum and minimum absorption of the protonated form. These values are listed in Table 2 and are in agreement with those reported previously [1].

Table 2
Spectral data of X as a function of pH

	λ_{\max} (nm)	λ_{\min} (nm)	
pH 2.0	325	260	$A_{1\%}^{1\text{cm}} = 340$
pH 12.0	356	279	$A_{1\%}^{1\text{cm}} = 672$

No significant differences were found between spectral data of X and Y; this is understandable since the N-1a substituent does not influence the chromophore.

pK_a determination

The anionic character of X has been demonstrated by its chromatographic behaviour. The pK_a value of the ionizable group was determined titrimetrically by monitoring the absorbance at 365 nm as a function of acidity. Where the pH was 3.5 or greater, degradation of X was too slow to interfere with the change in absorbance due to protonation. However, below pH 3.5 at 25°C the absorbance at 365 nm decreased continuously; this result can be attributed to decomposition. Nevertheless, the absorbance-pH curve was sufficiently complete to enable the pK_a value to be derived graphically as the inflection point of the titration curve. The pK_a value of 4.15 is comparable with those found for enolic hydroxyl groups [4].

Infrared spectroscopy

Infrared spectra of an isolated and derivatized degradation product provides only limited structural information. In the spectra of acetylated Y, for example, an absorption peak at 1775 cm⁻¹ is present whereas this peak is absent from the spectra of the parent mitomycins. This absorption can be attributed to the enolic acetate group ($\nu_{\text{C=O}}$) [5]. A strong band is present in the region near 1720 cm⁻¹; this band may be the result of carbamate absorption as well as that of the quinone carbonyl functions.

Polarography

At pH 8 the $E_{1/2}$ of the first reduction step, which corresponds to uptake of two electrons, is -425 mV for X, compared with -405 mV for MMC.

Mass spectroscopy

As previously found for synthetic mitosenes [6], acetylated mitosenes [7] and mitosane analogues [8], electron impact (EI) mass spectrometry appeared to be a useful tool for determination of the structure and for identification of this class of compounds. Good agreement was found between the EI mass spectra of the four reference compounds MMA, MMB, MMC and PM and those in earlier reports [8].

It appears that no MS studies of 7-hydroxymitosanes have been published. Apart from low volatility, 7-hydroxymitosanes degrade to 7-hydroxymitosenes upon protonation and therefore the hydroxyl function must be derivatized. Because of the greater stability of the resulting derivative protonation was preferred to acetylation in most instances. Under the chosen conditions the aziridine nitrogen of MMC is also derivatized, unlike the tertiary nitrogen of PM.

In the high mass region, FD-MS and CI-MS provide most information. EI-MS gave weak or no parent ions but led to more complicated fragmentation patterns.

FD-MS allows characterization of the intact molecule. M^+ , MH^+ and/or MNa^+ ions were observed in the FD mass spectra of the parent mitomycins as well as those of the acetylated or propionated 7-hydroxymitosanes. These masses were in agreement with the assigned structures.

CI-MS has never been used for the analysis of mitosanes. Isobutane CI-MS was used by Andrews and co-workers [7] for determination of the structure of acetylated mitosanes, but that technique was found to offer no advantage over EI-MS.

In the present study methane CI-MS was used and this technique appeared to be of value for the structural characterization of derivatized 7-hydroxymitosanes, especially in the high mass region. Protonated molecular ions were always present. In all analyses the characteristic masses of $(M + 29)$ and $(M + 41)$ were observed. It appears that the mitomycins have a great affinity towards components ($C_2H_5^+$, $C_3H_5^+$) from the ionizing gas under the chosen MS conditions. The four reference compounds showed an analogous fragmentation pattern of $[M^+ - H_3COH]$, $[M^+ - \cdot O_2CNH_2]$ and $[M^+ - H_3COH, \cdot O_2CNH_2]$.

For MMB, H_2O was eliminated instead of H_3COH . The fragments described above were also found in the spectra of the derivatized 7-hydroxymitosanes. EI mass spectra of the four reference compounds, as for the derivatized 7-hydroxymitosanes, mostly lacked parent peaks.

Fragmentation pathways of MMA, MMB, MMC and PM [8] and acetylated mitosanes [7] have been reported previously. The EI-MS behaviour of the acetylated and propionated 7-hydroxymitosanes shows some resemblance to the behaviour of these compounds. The fragmentation pattern of propionated Y (M405) may serve as a representative example.

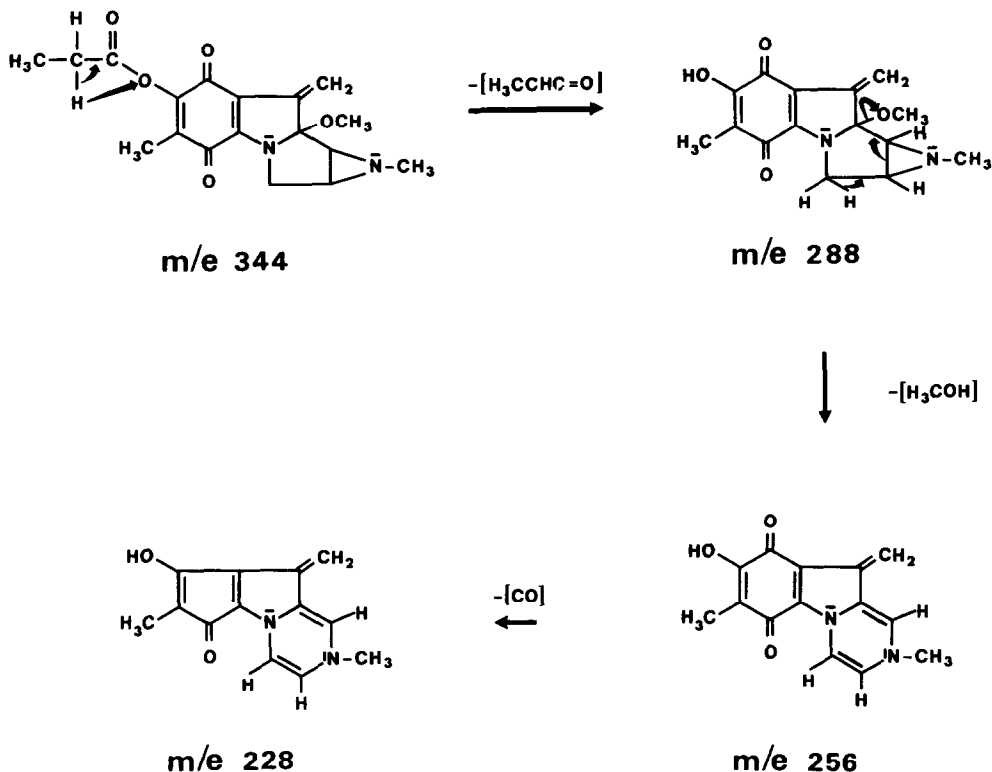
From the molecular ion methanol is eliminated and gives rise to m/z 373. Loss of carbamic acid corresponds to the next fragment ion m/z 344 that possesses a double bond between C_9 and C_{10} (Fig. 3). Subsequent cleavage of a methyl radical with loss of 15 mass units (m.u.) may give rise to fragment m/z 329. The mass of 288 may arise from the loss of a ketene group (56 m.u.) from fragment m/z 344 (Fig. 3). Elimination of a methyl radical from this fragment may lead to the second most abundant ion, m/z 273.

The most intense ion in the high mass region is m/z 256. This fragment may originate from the loss of methanol from m/z 288 (Fig. 3). Subsequent splitting of carbon monoxide and a methyl radical may explain the presence of fragments m/z 228 and m/z 213, respectively. In the low mass region the m/z values 83, 69, 57, 44 and 32 were observed.

Decomposition of MMC at pH > 13

Hydrolysis of the 7-amino groups of MMC and PM occurs in the pH region 8–13, whereas the remainder of the molecule remains intact. By means of HPLC (mobile phase III) and absorption spectrophotometry it was observed that MMC degrades to give another product (P_1) at pH values over 13.

This reddish compound appears to have spectral and chromatographic properties similar to those of the first degradation product of X formed under the same conditions. These data might suggest the possibility of a consecutive reaction in which MMC degrades to X, which then undergoes further degradation. However, when the degradation processes are followed spectrophotometrically the results do not support this hypothesis.

**Figure 3**

Proposed electron impact fragmentation pathway of $m/z\ 344$ originating from protonated Y.

Figures 4, 5 and 6 represent the curves of the spectral changes of, respectively, MMC, X and P_1^x in 2.0 M sodium hydroxide ($H_0\ 14.3$) at 25°C.

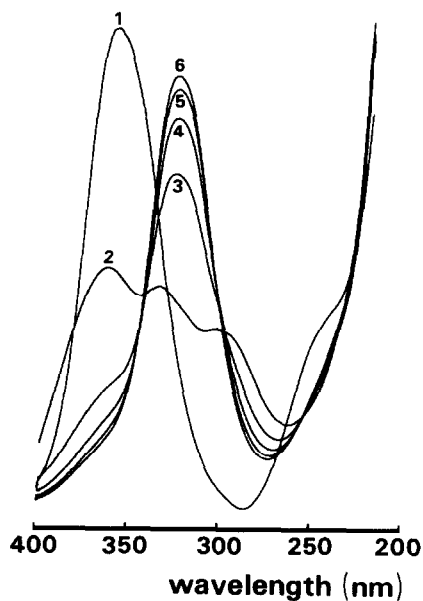
Underberg and Lingeman [9] observed a rapid change in absorptivity at 363 nm at pH values greater than 10.4 and attributed this phenomenon to keto-enol tautomerism in the quinoid moiety of the MMC molecule, stabilized by deprotonation. The pK_a of the acidic function was 12.44 [9]. In Fig. 4, curve 1 represents the absorbance of MMC in water. Spectral curve 2 can be attributed to the deprotonated form of MMC and subsequent curves to decomposition of this species. This also explains why curve 1 does not intersect the isosbestic point at 343 nm, associated with the conversion of deprotonated MMC into P_1 . An analogous observation was made in the decomposition of deprotonated X under the same conditions (Fig. 5).

When the change in absorptivity at 365 nm of deprotonated X in 2.0 M sodium hydroxide is monitored continuously, the resulting curve can be divided into two parts. A very rapid decrease occurs during the first 60 s; after 60 s the change in absorptivity is relatively slow and can be attributed to decomposition that follows first-order kinetics. It is possible that transformation of deprotonated X into a mesomeric form is favoured in the strongly alkaline medium. This could be an explanation for the observation that curve 1 in Fig. 5 does not intersect the isosbestic point at 338 nm.

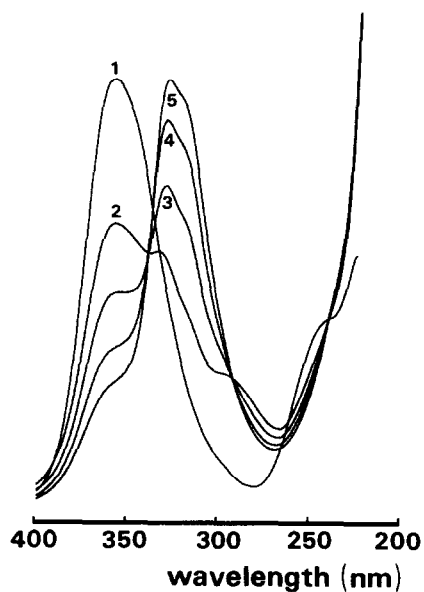
Curve 2 may partially represent the favoured mesomeric form, which in turn decomposes to P_1^x and results in the isosbestic points at 338 nm and 292 nm. Since the

Figure 4

Ultraviolet spectra of 3×10^{-5} M MMC in water (1) after the start of degradation in 2.0 M sodium hydroxide (H₂ 14.3); and (2), $t = 20$ s; (3), $t = 3.5$ min; (4), $t = 6.5$ min; (5), $t = 9.75$ min; (6), $t = 13$ min. Temperature, 25°C.

**Figure 5**

Ultraviolet spectra of 3×10^{-5} M X in water at pH 10 (1) after the start of degradation in 2.0 M sodium hydroxide (H₂ 14.3); and (2), $t = 1$ min; (3), $t = 4$ min; (4), $t = 8$ min; (5), $t = 12$ min. Temperature, 25°C.

**Table 3**

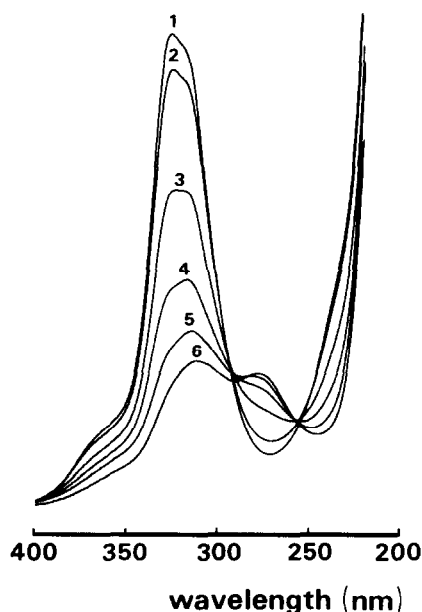
Isosbestic points related to the conversions of MMC, P₁, X and P₁^x in 2.0 M sodium hydroxide at 25°C

MMC → P ₁	343	299	Fig. 4
P ₁ → P ₂	292	256	
X → P ₁ ^x	338	292	Fig. 5
P ₁ ^x → P ₂	292	256	Fig. 6

x = Originating from X.

Figure 6

Ultraviolet spectra of P_1^\ddagger originating from X after the start of the degradation of X in 2.0 M sodium hydroxide (H₂ 14.3): (1), $t = 30$ min; (2), $t = 90$ min; (3), $t = 240$ min; (4), $t = 390$ min; (5), $t = 570$ min; (6), $t = 1230$ min. Temperature 25°C.



isosbestic points (Table 3) observed during the degradation of deprotonated MMC and X are significantly different, it may be inferred that deprotonated MMC degrades without X being formed as an intermediate, although the same degradation product P_1 (or P_1^\ddagger originating from X) is formed. This implies that the molecular structure of MMC^- undergoes simultaneous degradation at more than one site including the 7-position. Further degradation of P_1 or P_1^\ddagger leads to products in which the chromophore is changed dramatically; this change is demonstrated by the lack of absorbance (Fig. 6, curve 6).

The instability of the quinoid chromophore is also observed when 1,4-benzoquinone is examined in a strongly alkaline medium [10]. No attempts were made to elucidate the structures of P_1 or P_2 because of the minor importance of these compounds which are formed only in a strong alkaline medium. Work in progress may cast further light on these degradative processes.

References

- [1] E. R. Garrett, *J. Med. Chem.* **6**, 488–501 (1963).
- [2] E. R. Garrett and W. Schroeder, *J. Pharm. Sci.* **53**, 917–923 (1964).
- [3] W. Schroeder, U.S. Pat. 3, 306, 821 (1967).
- [4] *The Merck Index*, 9th Edn., pp. 8887. Merck, Rahway, NJ (1976).
- [5] L. J. Bellamy, *The Infra Red Spectra of Complex Molecules*, 3rd Edn, pp. 207–208. Chapman & Hall, London (1975).
- [6] J. Hodges, K. H. Schram, P. F. Baker and W. A. Remers, *J. Heterocyclic Chem.* **19**, 161–165 (1982).
- [7] P. A. Andrews, S.-S. Pan and N. R. Bachur, *J. Chromatogr.* **262**, 231–247 (1983).
- [8] G. E. Van Lear, *Tetrahedron* **26**, 2587–2597 (1970).
- [9] W. J. M. Underberg and H. Lingeman, *J. Pharm. Sci.* **72**, 553–556 (1983).
- [10] P. Hodge, in *The Chemistry of the Quinoid Compounds* (S. Patai, Ed.), pp. 579–613. John Wiley, London (1974).

[First received for review 24 July 1984; revised manuscript received 4 October 1984]